Earthquakes and Structures, *Vol. 22, No. 2 (2022) 121-135*
https://doi.org/10.12989/eas.2022.22.2.121

Experimental assessment of post-earthquake retrofitted reinforced concrete frame partially infilled with fly-ash brick

Sanjay R. Kumawat[a], Goutam Mondal* and Suresh R. Dash[b]

School of Infrastructure, Indian Institute of Technology Bhubaneshwar, Jatni, Odisha 752050, India

(Received June 29, 2021, Revised October 2, 2021, Accepted October 12, 2021)

Abstract. Many public buildings such as schools, hospitals, etc., where partial infill walls are present in reinforced concrete (RC) structures, have undergone undesirable damage/failure attributed to captive column effect during a moderate to severe earthquake shaking. Often, the situation gets worsened when these RC frames are non-ductile in nature, thus reducing the deformable capability of the frame. Also, in many parts of the Indian subcontinent, it is mandatory to use fly-ash bricks for construction so as to reduce the burden on the disposal of fly-ash produced at thermal power plants. In some scenario, when the non-ductile RC frame, partially infilled by fly-ash bricks, suffers major structural damage, the challenge remains on how to retrofit and restore it. Thus, in this study, two full-scale one-bay, one-story non-ductile RC frame models, namely, bare frame and RC partially infilled frame with fly-ash bricks in 50% of its opening area are considered. In the previous experiments, these models were subjected to slow-cyclic displacement-controlled loading to replicate damage due to a moderate earthquake. Now, in this study these damaged frames were retrofitted and an experimental investigation was performed on the retrofitted specimens to examine the effectiveness of the proposed retrofitting scheme. A hybrid retrofitting technique combining epoxy injection grouting with an innovative and easy-to-implement steel jacketing technique was proposed. This proposed retrofitting method has ensured proper confinement of damaged concrete. The retrofitted models were subjected to the same slow cyclic displacement-controlled loading which was used to damage the frames. The experimental study concluded that the hybrid retrofitting technique was quite effective in enhancing and regaining various seismic performance parameters such as, lateral strength and lateral stiffness of partially fly-ash brick infilled RC frame. Thus, the steel jacketing retrofitting scheme along with the epoxy injection grouting can be relied on for possible repair of the structural members which are damaged due to the captive column effect during the seismic shaking.

Keywords: captive column effect; epoxy injection grouting; fly-ash infill; full-scale experiment; partial infill wall; retrofitting; steel jacketing

1. Introduction

Partial infill walls are normally present in the schools, hospitals, and other public buildings to fulfill the functional and aesthetic requirements, in the form of openings, doors, windows, ventilators, etc. Nowadays to reduce the environmental impact, the infill walls are constructed using fly-ash bricks in place of traditional burnt clay bricks, and also laws on the use of fly-ash bricks has been enforced in many parts of Indian subcontinental region close to thermal power plants. Most of these existing reinforced concrete (RC) buildings located in the Indian subcontinent region are non-ductile in nature and stand a high chance to suffer damages during a moderate earthquake, especially in presence of partial infill masonry walls. The presence of partial infill wall in non-ductile RC frames accelerates undesirable modes of failure such as captive column effect (Muduli *et al.* 2020), as seen in many past earthquakes. Nevertheless, it is observed in the literature that the softening of bracing action due to partial infill wall makes the building frame more vulnerable to out-of-plane loading (Yuen *et al.* 2016). Such structures, damaged in an earthquake, have to be repaired economically and efficiently within limited time as emergency infrastructures like hospitals, schools need to be resumed at the earliest. However, to the best of the authors' knowledge, no study was found in literature for retrofitting of damaged non-ductile RC frame, partially infilled with fly-ash brick masonry. Therefore, the present study tries to address this aspect with a novel easy-to-implement retrofitting scheme.

Many past experimental studies, available in the literature, provide retrofitting schemes for various RC frames and frame members including beam-column joint. Some of the major experimental studies related to both strengthening and repairing schemes of infilled frames and beam-column joints have been reviewed to come up with the best possible scheme applicable to non-ductile partially infilled RC frames.

Many researchers have contributed to the strengthening of seismically deficient RC frames with infill walls (Altin *et al.* (2008), Yuksel *et al.* (2010), Kumbasaroglu *et al.* (2016),

*Corresponding author, Assistant Professor
E-mail: gmondal@iitbbs.ac.in
[a]M.Tech. Scholar
E-mail: srk11@iitbbs.ac.in
[b]Ph.D. Assistant Professor
E-mail: srdash@iitbbs.ac.in

ISSN: 2092-7614 (Print), 2092-7622 (Online)

Srechai *et al.* (2017), Darbhanzi *et al.* (2018), Soltanzadeh *et al.* (2018), and Ro *et al*. (2020)). Altin *et al*. (2008) introduced CFRP bracings with sheets as cross bracing to strengthen the wall of a 1/3 scale, one-bay, one-storey perforated clay brick-infilled nonductile RC frames. They found that after a certain thickness of cross-bracing, the variation in the strength of the infill wall was stopped. Yuksel *et al*. (2010) used different arrangements of Carbon Fibre Reinforced Polymer (CFRP) bracings such as diamond bracing, cross bracing, cross-diamond bracing, and off-diagonal bracing for the strengthening of unreinforced masonry infill wall and compared them with infilled and bare frame specimen. All the strengthened specimens showed improved strength and rigidity parameters. The cross-diamond braced specimen showed a gradual reduction in its strength and a better energy dissipation capacity than the others. Kumbasaroglu *et al.* (2016) experimentally investigated the effect of anchorage bars on 1:4 scaled concrete infilled steel frames. The results revealed that anchorage bars significantly increased the initial stiffness and energy dissipation capacity of the steel frame than the unanchored steel frame. Srechai *et al*. (2017) carried out experimental investigation on large scale non-ductile masonry infilled RC frames to evaluate the effectiveness of a proposed strengthening scheme. A vertical gap with small vertical steel members was introduced between the masonry infill and the column to reduce the direct shear on the columns and wire meshes and high strength mortar was used in the areas of high stresses. The retrofitted infilled RC specimens performed well. While, Darbhanzi *et al*. (2018) enhanced the strength and ductility of unreinforced masonry walls by using vertical and diagonal steel strips. The experiment results showed that there was a significant increase in seismic capacity showing an 200% increment in strength and 20% increment in displacement capacity. Soltanzadeh *et al.* (2018) experimentally verified the seismic retrofitting of 1:3 scaled RC frames fully infilled with clay bricks using two different aspect ratios of frames (height/length ratio of 0.5 and 1). The retrofitting method includes the use of post-tensioned bars to prevent premature failure in the infill wall. The retrofitting frames showed higher strength and stiffness values for the frames, with a gradual reduction in its initial stiffness. Ro *et al*. (2020), has experimentally investigated the effect of welded concrete filled steel tubes on seismic performance of RC frames. The retrofitting scheme was effective, economic and the structure can be occupied even during the construction period.

A very limited work has been focused on the strengthening of RC frames with partial infill wall. Jayaguru and Subramanian (2012) strengthened an undamaged partially infilled RC frame by using Glass Fiber Reinforced Polymer (GFRP) wrapping around the mid-height of the column to eliminate the captive column failure. The experimental results showed a gradual failure of the specimen as compared to the original unstrengthened frame. The shifting of captive failure was observed from the mid-height of the column to a lower height.

Studies have been also carried out in the past on the strengthening of non-ductile RC beam-column joints (El-Amoury *et al.* (2002), Hadi *et al.* (2014), Chang *et al.* (2014), Hadigheh *et al.* (2014)). El-Amoury *et al.* (2002) have performed strengthening of the beam-column joint with inadequate anchorage, by welding the beam bars with a steel angle attached at the corner of the joint and then GFRP sheets were wrapped to confine the beam-column joint. This retrofitting technique increased the overall capacity of the beam-column joint but the welding of beam bars with column bars led to buckling of the column bars. Hadi *et al.* (2014) carried out the strengthening of non-ductile exterior beam-column joint using the Carbon Fiber Reinforced Polymer (CFRP) jacket and found that the retrofitting was effective when the square cross-section of the column was transformed to a circular one by gluing rounded concrete covers on all the four sides prior to the wrapping of CFRP jacket. Chang *et al.* (2014) carried out an experimental investigation on three half scaled retrofitted specimens of RC columns. The Super Reinforcement with Flexibility retrofitting scheme was adopted for strengthening the columns which increased its strength and ductility. Hadigheh *et al.* (2014) performed experimental studies on the strengthening of a scaled model (1:2.2) of the eight-story building frame by using Fiber Reinforced Polymer (FRP) sheets at the beam-column joint region. They found that the FRP retrofitting showed better seismic performance than the steel bracing.

Researchers were also actively involved in developing repair techniques for RC frames. However, the focus was mainly on repairing of the beam-column joints. Faleschini *et al.* (2019) compared the repair technique of non-ductile beam-column joint damaged due to cyclic loading by using FRP and Fiber Reinforced Cementitious Matrix (FRCM). The specimen retrofitted with FRCM was found to perform better than FRP specimens in terms of strength, although it showed a poor performance in terms of energy dissipation capacity. Tsonos (2008) has done a comparative study between the RC jacketing and CFRP jacketing on a beam-column joint assemblage. The shifting of plastic hinge formation was observed in both cases. Sasmal *et al.* (2011) have carried out an experimental repair work of beam-column joint using steel plates which were applied using five anchor bolts and L-shaped GFRP layers at the corner of the beam-column joint. This technique was effective in restoring the strength provided that internal cracks were filled, and the loose concrete was replaced with new concrete. Garcia *et al.* (2014) have replaced the damaged concrete from the joint region of the non-ductile beam-column joint with new concrete and wrapped it with CFRP sheets to retrofit the joint. The cyclic loading test on the repaired specimen showed 44% increase in its shear strength. Karayannis *et al.* (2018) carried out an experimental investigation on ten full scaled damaged beam-column joints after repairing them with CFRP sheets along with thin resin inclusion in to the cracks. The technique proved to be satisfactory for mild to moderately damaged beam-column joints.

Thus, to the best of authors knowledge, no experimental study has been carried out involving the repair techniques for damaged partially infilled RC frames after an earthquake. A clear need of development of a retrofitting

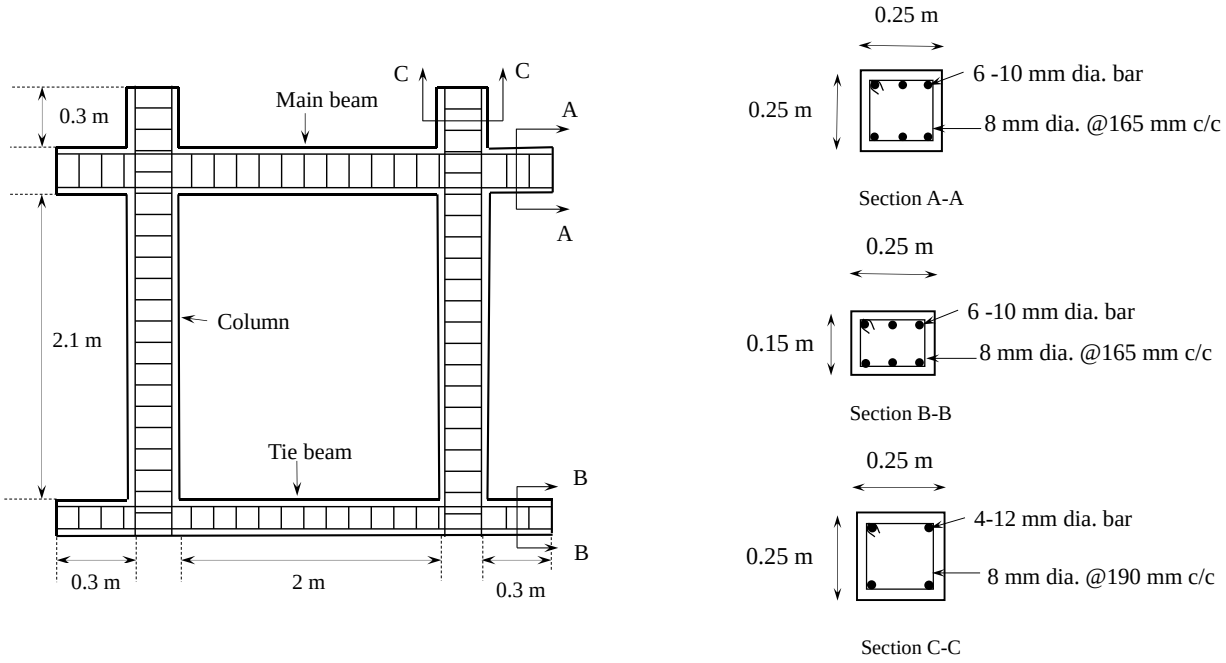

Fig. 1 Reinforcement details and frame dimensions of the RC frame

scheme is evident for post-earthquake damaged partially infilled RC frames. Hence, in this study, a full-scale experimental investigation has been carried out on the post-earthquake retrofitted partially fly-ash brick infilled frame. The retrofitting scheme is developed with the aim of fast and speedy implementation on the damaged structure with the aim of regaining the original undamaged lateral strength and lateral stiffness of the RC frames, so that the structure can be reused as early as possible after an earthquake.

Table 1 Notations of the type of frames considered in this study

Notation	Type of frame
BF	Undamaged bare frame
PIF	Undamaged partially infilled frame with fly-ash brick masonry
DBFR-G	Damaged bare frame (BF) retrofitted with epoxy grout
DPIFR-GS	Damaged partially infilled frame (PIF) retrofitted with epoxy grout and steel jacket and partially infilled with new fly-ash brick masonry

2. Details of damaged RC specimens

In the present experimental study, two full-scale models of RC frames (Table 1), one bare frame, i.e., without infill (BF) and one with partially infilled frame (PIF) damaged during the previous experimental program conducted by Kaushik *et al.* (2018) are considered for retrofitting. Both the RC frames have identical geometric configuration, as shown in Fig. 1. The specimens considered were representative of non-ductile frames taken from the ground story of a three-bay two-story RC non-ductile building frame. The specimens were designed as per the Indian Standard *IS 456-2000 (BIS, 2000)*, without any provision of ductile detailing. The RC frame considered in this study, consists of a main beam at the lintel level, a bottom tie beam along with the columns (Fig. 1). The openings usually present in the RC frames widely varies between 20-80% of the full infill wall, which are provided in the corridors/rooms of schools, hospitals, and other public buildings for various functional requirements. For the present study, a RC frame with partial infill wall (using fly-ash brick masonry) covering 50% of the opening is considered, that typically represent the opening in the RC frames at the ground floor level of a three bay two story school building. The beam and the columns have been casted with 300 mm projections to have adequate bond length (through development length) between concrete and steel reinforcement. The reinforcement details and the dimensions of the frames is shown in Fig. 1. For a typical RC column section, it is well known that the flexural capacity increases with initial increase in axial load but decreases thereafter. Also, it is very rare for a midrise building to suffer tensile stresses in addition to gravity load during an earthquake. Thus, conservatively, no axial force was applied on the columns, and the major focus of the study remained in evaluating its capacity in flexural and shear failure modes. The bottom tie beam having its displacement restricted due to the floor and ground below is considered to be fixed.

Therefore, in the experiment, this tie beam was fixed to the strong concrete floor using anchor bolts. Figs. 2-3 show the damaged specimen considered in this study. The bare frame (BF) has suffered damages due to the formation of hinges near the beam-column joints (Fig. 2). In addition to the formation of hinges near the beam-column joints, the partial infilled frame (PIF) has suffered shear failure due to the captive-column effect at the mid-height of the column

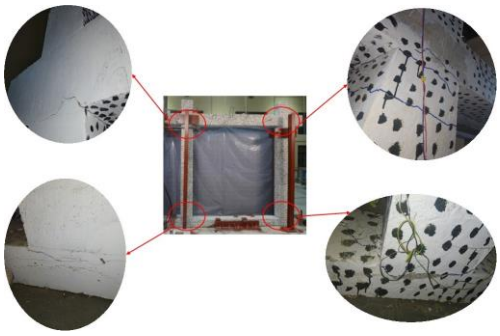

Fig. 2 RC non-ductile bare frame subjected to slow-cyclic loading (Kaushik *et al.* 2018)

Fig. 3 Damages to RC partial infill frame subjected to slow-cyclic loading (Kaushik *et al*. 2018)

(Fig. 3). The ultimate lateral strength of the bare frame (BF) and partially infilled frame (PIF) was 33.3 kN and 72.7 kN, respectively, whereas the secant stiffness (corresponding to 75% of the ultimate load (Park 1989)) of the frames is 2.17 kN/mm and 3.77 kN/mm in case of the BF and PIF, respectively.

Two different types of retrofitting schemes were adopted for these specimens. These include (a) DBFR-G: - Damaged RC bare frame (i.e., damaged BF) retrofitted with epoxy injection grouting and (b) DPIFR-GS: - Damaged RC frame partially infilled with fly-ash bricks (i.e., damaged PIF) retrofitted with epoxy injection grouting and steel jacketing retrofitting scheme. In the latter scheme, the whole wall was demolished and replaced by a new wall made of fly-ash bricks and mortar. The fly-ash bricks being made from industrial waste, are environment friendly. Also, due to its smooth finish and uniform size, it consumes about 40-50% less mortar, because of which it is gaining popularity over clay bricks. Further, an innovative technique of steel jacketing retrofitting scheme has been proposed for damaged RC structures, which ensures proper confinement of damaged concrete with the steel jackets. An experimental investigation on the retrofitted specimens was carried out by conducting the same slow cyclic displacement-controlled loading test which was conducted on undamaged specimen by Kaushik *et al*. (2018). The gain in various seismic parameters such as lateral strength, lateral stiffness, energy dissipation, and ductility of the retrofitted specimen was investigated from the experimental study.

3. Retrofitting of the bare frame (DBFR-G)

Visual inspection of the damaged frame (BF) was done thoroughly to ensure the possible location of the damage. To identify the damaged locations, the RC frames were struck with a hammer at various places. The striking or hitting of hammer was done with a low intensity force, just to check the hollowness in the specimens due to internal cracks. This process of identification of damaged location is identical to the soundness test, which is used to find the nature of the bricks. A distinct ringing sound would indicate that the concrete is sound, whereas a dull and hollow sound is an indication of cracked or de-bonded concrete. After the identification of damaged concrete locations, the loose concrete was removed by using a hammer and a chisel. The exposed concrete was cleaned by using a wired brush and an air blower. Injection nozzles of diameter 1.5 cm made of PVC material are installed at their desired locations to inject the epoxy resin. Depending on the extent of damage, about two to three nozzles were inserted at a particular damaged location. These nozzles were interconnected with each other by means of cracks. The epoxy grout was used as a sealant to seal the cracks along its length after installing the nozzles. The epoxy grout is a thick paste which is prepared by mixing stone dust powder with epoxy resin. Following the manufacturer recommendation, the epoxy resin was prepared by mixing epoxy components A and B in the ratio of 2:1.

Once the epoxy grout was applied to the damaged frames, it was allowed to dry for a period of about 24 hours. The epoxy resin was then injected through the installed injection nozzles with the help of a conical pressure vessel to fill the internal cracks of damaged RC frames. The conical pressure vessel was connected to a 2850 rpm capacity air compressor at one of its ends, which gave pressurized epoxy resin output at the other end. The pressurized epoxy resin was injected through the installed nozzle, and the flow of resin from the adjacent nozzle would indicate that the cracks between these two nozzles were filled entirely, and after that, these nozzles were sealed or packed. The resin was allowed to set for a period of 24 hours.

4. Retrofitting of the partially infilled frame (DPIFR-GS)

The partial infill wall of the damaged frame (PIF) was removed before initiating the repair work. The frame is then retrofitted using epoxy grout and resin as has been done for BF and left for 14 days for curing. After curing is done, the damaged locations are retrofitted by a jacketing technique using steel plates of thickness 1.5 mm. Steel plates were applied only at the damaged parts of the frame, i.e., at beam-column joints, mid-height of the column where captive column failure occurred, column ends where plastic hinges formation took place and at the base-beam column joint as shown in Fig. 4(a). The thickness of the steel plate used for retrofitting is decided based on the numerical analysis carried out by Kumawat *et al*. (2020). The

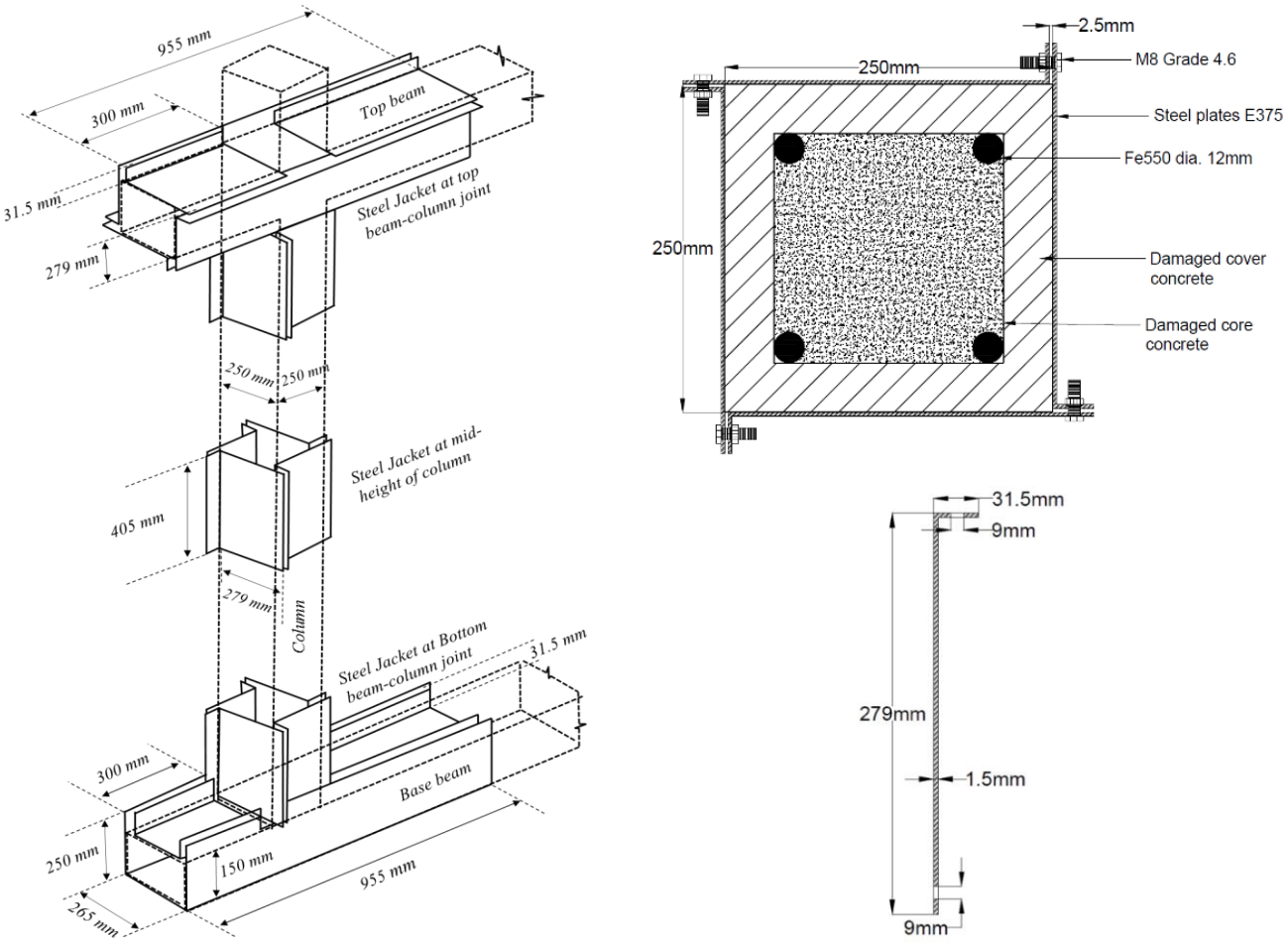

(a) (b)

Fig. 4 (a) Schematic diagram of steel jacketing of DPIFR-GS frame (b) Four side bolting of L-plates

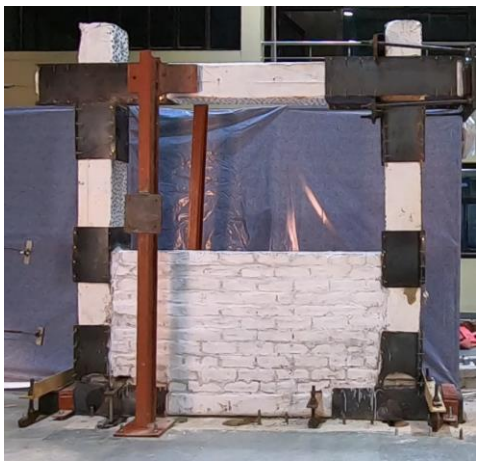

Fig. 5 Retrofitted partially infilled frame (DPIFR-GS)

numerical analysis shows that for 1.5 mm steel plate thickness, the ultimate lateral strength and lateral stiffness of the retrofitted partial infilled frame are 120% and 95% of its undamaged stage, respectively. For plate thicknesses higher than 1.5 mm, the partially infilled frame didn't show any significant increase in its strength and stiffness.

The repaired frame (with epoxy resin) and the externally applied steel plates should behave as an integrated system without any slippage between the two. For this purpose, four L-shaped plates were attached at the surfaces of damaged locations by using the epoxy adhesive and immediately bolted (before the curing was done) with each other by using M8 bolts to confine the concrete as shown in Fig. 4(b). A gap of 2.5 mm was kept initially between the short and the long legs of the adjacent L-shaped plates (Fig. 4(b)), so that the plates can confine the concrete cross-section when the bolts were tightened, by bending around its corner. The diameter of the bolt hole, the pitch and the edge distance of all the steel plates were maintained as 9 mm, 105 mm and 45 mm, respectively. However, the L-shaped plate arrangement was practically not viable for the tie beam. Hence, U-shaped plates were used, as shown in Fig. 4(a) for the tie beam. The U-shaped plate at the bottom beam was welded with the plates at the bottom of the column. Fig. 4(a) also shows the arrangement of plates at the top beam-column joint and at the top of the masonry infill wall, respectively. After the application of steel plates, the partial infill wall was constructed using fly-ash bricks used previously in the case of PIF, and the captivity in the columns was also kept same by constructing the wall in 50% of the opening area. The wall was thus cured for a period of 28 days thereafter. Fig. 5 shows the steel-jacketed partially infilled RC frame.

Table 2 Properties of the materials used in the retrofitted frames

Material	Property	Tested as per Code	Specimen size	Value (MPa)
Concrete cube	Compressive strength at 28 days	IS:516-1959 (BIS 1959)	150 mm × 150 mm × 150 mm	28.4
Steel reinforcement	Yield strength of steel	IS:1608-2005 (BIS 2005)	10mm dia. 12mm dia.	543 557
Brick unit	Compressive strength	IS:3495-PART 1-1992 (BIS 2005)	250 mm × 120 mm × 80 mm	10.5
Masonry prism	Compressive strength at 72 days (day of testing)	IS:1905-1987 (BIS 1987)	Four layers	6.28
Mortar cube	Compressive strength at 72 days (day of testing)	IS:4031-PART 6-1988 (BIS 1988)	70.6 mm × 70.6 mm × 70.6 mm	11.35
Epoxy cubes	Compressive strength at 72 days (day of testing)	ASTM C 579 (ASTM 2018)	150 mm × 150 mm × 150 mm	58
SIKA 53 UF (A + B)	Compressive strength at 14 days	ASTM C 579 (ASTM 2018)	50 mm × 50 mm × 50 mm	50
SIKA 31 IN (A + B)	Compressive strength at 14 days	ASTM C 579 (ASTM 2018)	50 mm × 50 mm × 50 mm	65
Steel plates	Yield strength of steel	Provided by manufacturer	-	210

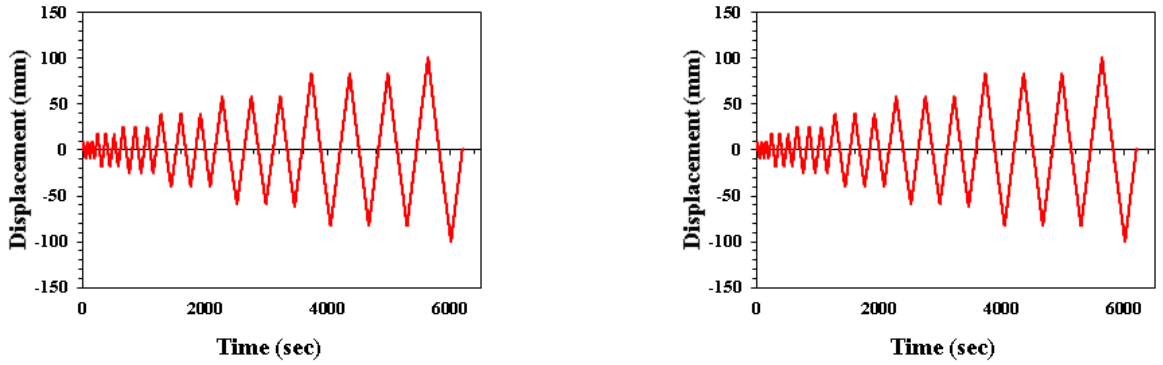

Fig. 6 (a) Time-history displacement plot for DBFR-G (b) Time history Displacement plot for DPIFR-GS

The properties of the epoxy resin and epoxy adhesive are provided by the manufacturer. The properties of the other materials are found from the test following corresponding Indian Standard codes. The average compressive strength of concrete was found to be 28.4 MPa. Also, a compressive strength test was conducted on three samples of 4 layered fly-ash brick prism to find the strength of the masonry wall. It was found that the average compressive strength of the masonry prisms is 6.28 MPa. The average strength of the epoxy grout was 58 MPa. The properties of the materials used for the retrofitting of the specimens are summarized in Table 2.

5. Experimental investigation of the retrofitted RC frames

Both the retrofitted specimens (DBFR-G and DPIFR-GS) were tested with the same loading history, as shown in Figs. 6(a)-(b) as applied to the respective undamaged frames (BF and PIF) by Kaushik *et al.* (2018). The rate of loading was maintained at 0.5 mm/sec throughout the experiments. The recording of experimental results was done by using a load cell and displacement transducer present at the actuator arm and external LVDT's using Data Acquisition System. The experimental setup for both the frames are shown in Figs. 7-8.

5.1 Hysteretic behaviour and failure modes of frame

The hysteresis response of the RC frames shows the variation of the lateral load with lateral displacement for each cycle of loading. The displacement-controlled loading was applied in three repetitive cycles of 10 mm, 20 mm, 30 mm, 50 mm, 75 mm, and 100 mm of maximum displacement at a rate of 0.5 mm/sec. The experiment was stopped once a significant (less than 70% of ultimate strength) decrease in the lateral load was observed with an increase in displacement.

5.1.1. Response of retrofitted bare frame (DBFR-G)

The hysteresis response of the retrofitted bare frame (DBFR-G) is shown in Fig. 9. For the 10 mm displacement cycle (at 0.4% drift), no significant change was observed in the frame, while for the 20 mm cycle (0.8% drift), the first crack was observed at the bottom of the leeward column. During the 30 mm cycle of loading (1.2% drift), multiple hairline cracks began to emerge at the top of the column just below the beam-column joint. The cracks started to enlarge at the top of the column in the 50 mm cycle of loading (2% drift) followed by the initiation of the plastic hinge in the tie beam, and the spalling of epoxy grout at the beam-column joints. But it is worthy to note that no cracks were formed at the epoxy grouted location as the epoxy sealant was stronger than the concrete used in this study

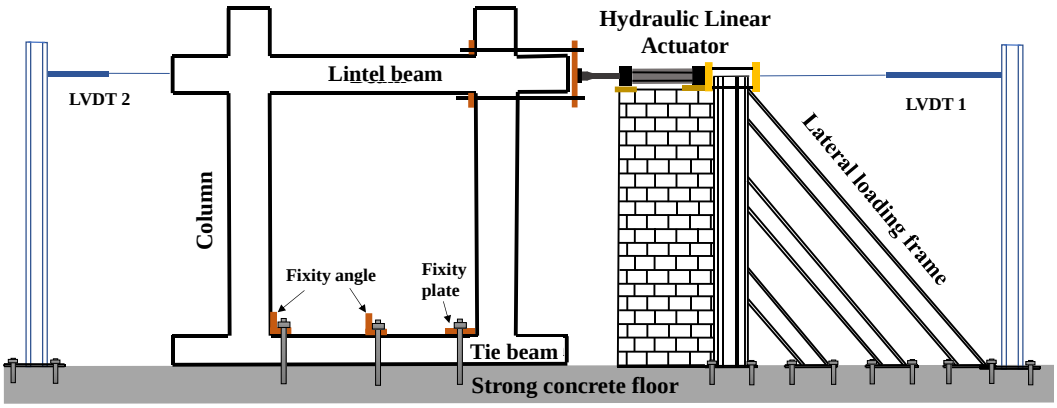

Fig. 7 Experimental setup of DBFR-G frame testing

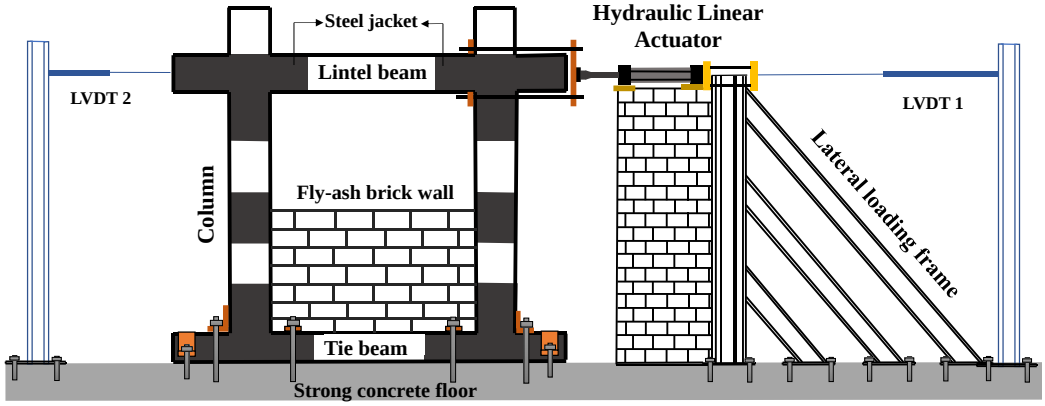

Fig. 8 Experimental setup of DPIFR-GS testing

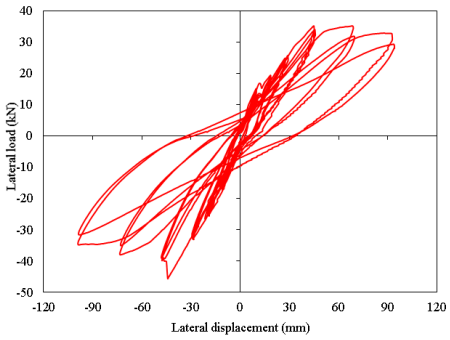

Fig. 9 Hysteresis response of the retrofitted bare frame (DBFR-G)

Fig. 10 Failure cracks in epoxy retrofitted bare frame (DBFR-G)

(Table 2). Therefore, the damages were shifted from the beam-column joint to the top of the column, as shown in Fig. 10. In the 75 mm cycle of loading (3% drift), the formation of hinges took place in the tie beam at the same locations (i.e., at bottom beam-column joint) as it was observed in BF by Kaushik *et al.* (2018). In the final cycle of 100 mm (4% drift), the cracks in the tie beam and column were enlarged, and the frame was no longer able to resist the further load. Similar failure was observed in the case of the bare frame tested by (Kumbasaroglu *et al.* 2017 and Basha *et al*. 2016), where the failure took place mainly due to the formation of hinges at the top beam-column joint and the bottom of the column.

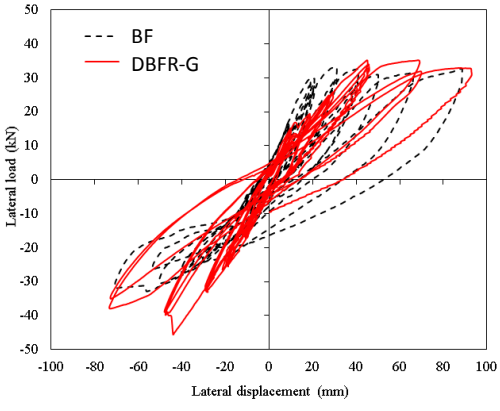

Fig. 11 Comparative hysteresis curve of the bare frame before and after retrofitting

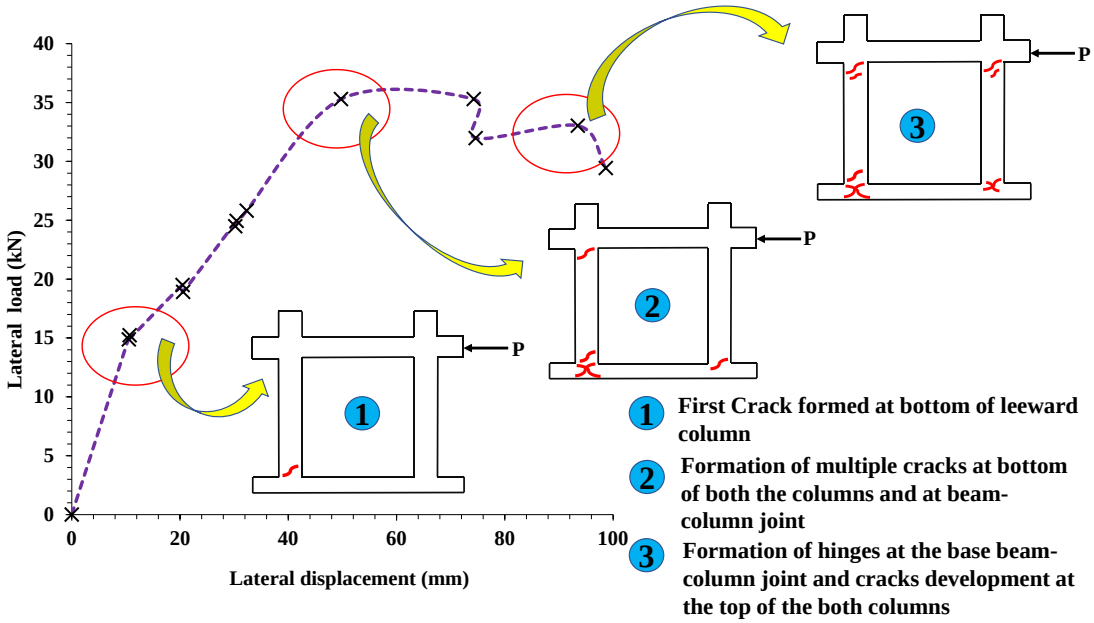

Fig. 12 Progressive failure of the retrofitted bare frame (DBFR-G) with increasing cycles of loading

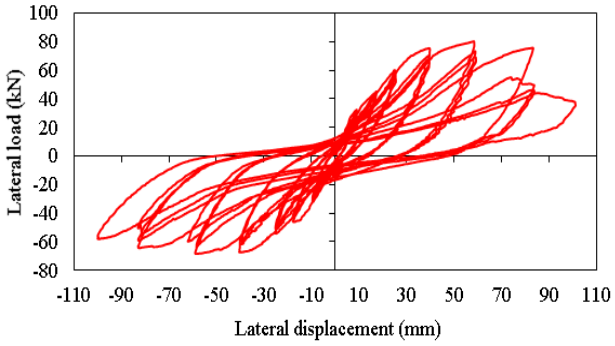

Fig. 13 Hysteresis response of DPIFR-GS frame

Fig. 14 Failure cracks in DPIFR-GS

The progressive failure of the retrofitted frame (DBFR-G) with an increasing cycle of loading is illustrated with the help of the backbone curve and is shown in Fig. 12. The initial stiffness of the frame suddenly dropped by 36% during the first 20 mm displacement cycle due to the formation of cracks at the bottom of the leeward column. After that, the stiffness almost remained constant with displacement. The frame attains its maximum lateral strength of 35 kN at the displacement cycle of 50 mm. At this stage of loading, multiple cracks are formed at the bottom beam-column joint, and at the top and bottom of the columns. Following that cycle of loading, the load-carrying capacity of the frame almost remains constant up to 75 mm displacement. The frame fails to resist more load in its final 100 mm displacement cycle due to the failure of the bottom beam-column joints and damages caused at the top of the columns. The comparative hysteresis curve of the undamaged bare frame (BF) and the retrofitted one (DBFR-G) is shown in Fig. 11 (for drift value of 3.6%). The BF shows more symmetric behavior (in pull and push loadings) as compared to the DBFR-G. A pinching effect has been observed during the pull loading (negative displacement cycle) of the specimen DBFR-G.

5.1.2. Response of retrofitted partially infilled frame (DPIFR-GS)

The hysteresis response of the DPIFR-GS frame is shown in Fig. 13. The separation of the masonry wall and the column was observed at a small frame displacement (20 mm cycle of loading, i.e., 0.8% drift) similar to the separation which was observed in the experiment conducted on infill frame without anchorage by Kumbasaroglu *et al.* (2016), Kumbasaroglu *et al.* (2017) and Basha *et al.* (2016). In the 30 mm cycle of loading (1.2% drift), the bed-joint failure was observed at the interface of the wall and tie beam followed by shear failure at column due to the captive column effect. The steel jackets seemed to be helpful in shifting the captive column failure from the mid-height towards the downward direction of the columns, as also observed by Jayaguru and Subramanian (2012). In the 50 mm displacement cycle (2% drift), the captive column failure was completely developed in both the columns, as shown in Fig. 14. When the displacement was increased to 75 mm (3% drift), bed-joint failure was observed in the second last bricklayer, during which the wall above the bottom two bricklayers was moving as an integrated block. At the final cycle of 100 mm displacement (4% drift), sudden bed-joint failure of the top most mortar layer was observed, and the welding of the U-plates with the bottom

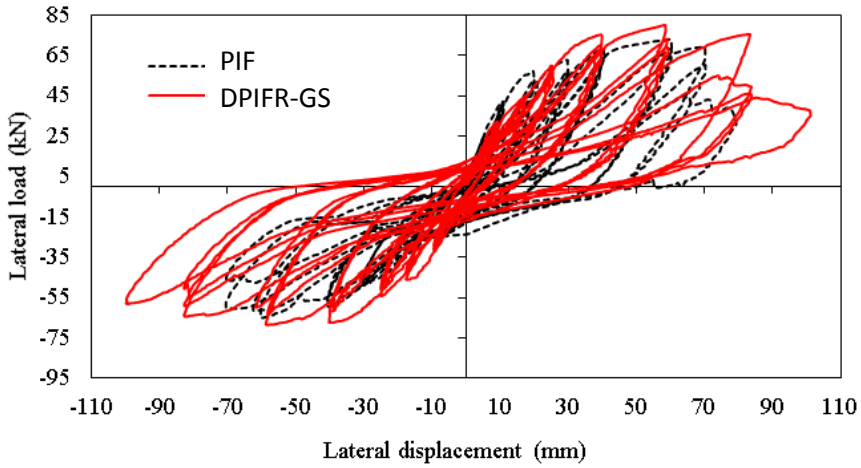

Fig. 15 Comparative hysteresis curve of PI frame before and after retrofitting

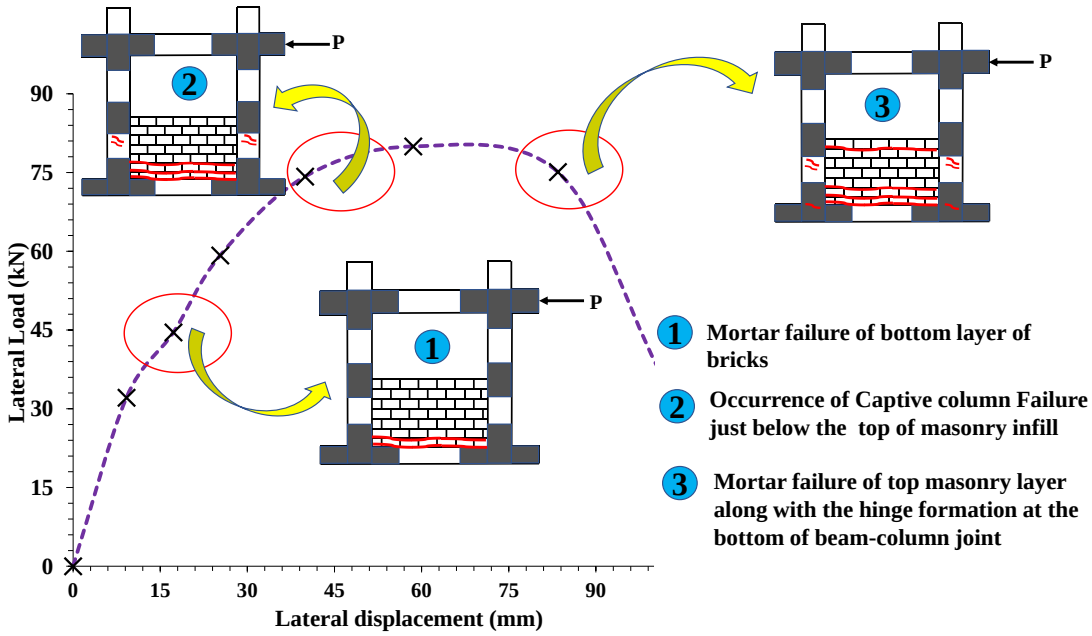

Fig. 16 Progressive failure of DPIFR-GS with increasing cycles of loading

plates of the column was ruptured and entirely separated in the windward column (Fig. 14), which led to the formation of hinges at the base beam-column joint thereby reducing the lateral strength of the frame drastically. Fig. 15 shows the comparative hysteresis curve of the partially infilled frame before and after retrofitting for 3.2% of drift value. Both PIF and DPIFR-GS showed symmetric behaviour in the push and the pull cycle.

The progressive failure of DPIFR-GS with the increasing cycle of loading is shown with the help of the backbone curve in Fig. 16. The initial stiffness drops by 30% due to the failure of bed-joint at the tie-beam wall interface at a 20 mm cycle of displacement (0.8% drift). The frame attained its capacity of 80 kN in the 50 mm cycle of displacement (2% drift), after which the load-carrying capacity remained constant due to the formation of captive column failure and sliding failure of bottom two bricklayers. The ultimate failure occurs during the 75 mm displacement cycle (3% drift), after which the load constantly drops due to the formation of hinges at the bottom beam-column joint.

5.2. Comparison of lateral strength of the undamaged and retrofitted frames

The lateral strength for displacement-controlled loading cycles was taken as the maximum of the three repetitive cycles, which is the strength of the first cycle in most of the displacements.

5.2.1. Lateral strength of DBFR-G

The maximum strength attained by the DBFR-G frame during the cyclic loading was 45 kN, which is 137% of the original strength of BF. However, when compared with the secant stiffness, it was found that DBFR-G has a maximum secant stiffness value of 1.13 kN/mm, which is 117% of the original stiffness of BF. Secant stiffness is calculated as the ratio of load corresponding to 75% of the ultimate load to

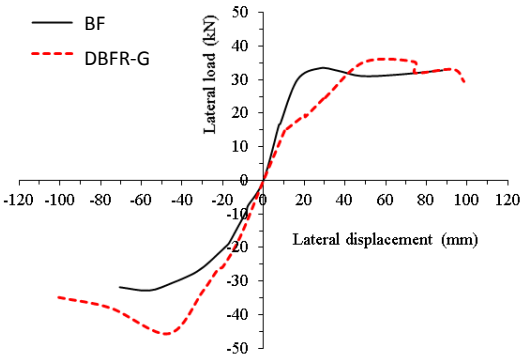

Fig. 17 Comparison of the backbone curves of the undamaged (BF) and damaged retrofitted (DBFR-G) bare frames

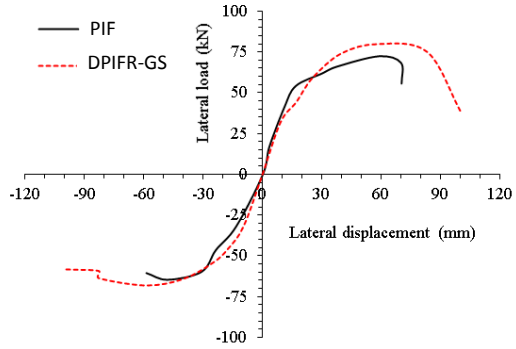

Fig. 18 Comparison of the backbone curves of the undamaged (PIF) and damaged retrofitted (DPIFR-GS) partial infill frames

the deformation at that load (Park 1989). The abrupt fall in the initial stiffness value of the frames during the 20 mm displacement cycle (both in undamaged and retrofitted bare frame case) is due to the crack formation in the bottom beam-column joint. Fig. 17 shows a comparative backbone curve of the BF and DBFR-G. It is observed that after 75 mm of positive displacement cycle, the curves closely overlap, which means that the failure of the frames followed a similar trend. However, the overall behaviour of DBFR-G is similar to that of BF.

5.2.2. Lateral strength of DPIFR-GS

The lateral strength of the DPIFR-GS is compared with the undamaged partially infilled frame (PIF) and with the numerical analysis of the DPIFR-GS specimen. Fig. 18 shows a comparative backbone curve of the PIF and DPIFR-GS specimens. The maximum strength of DPIFR-GS was found to be 80 kN, which is 111% of the strength of the undamaged frame (PIF). The secant stiffness of the two cases also showed a good match. The maximum secant stiffness of the DPIFR-GS was 2.34 kN/mm, which is 62% of the secant stiffness of the PIF. Table 3 shows the comparative strength and stiffness gain of retrofitted frames. Similar variation in lateral strength and stiffness in the push and pull loading was also observed by Esmaeeli *et al.* (2015).

Table 3. Lateral strength and stiffness of retrofitted frames

Specimen	Lateral strength (kN)				Lateral secant stiffness (kN/mm)			
	Push cycle	Error (%)	Pull cycle	Error (%)	Push cycle	Error (%)	Pull cycle	Error (%)
BF	33.3	0	32.8	0	2.1	0	0.96	0
DBFR-G	35.3	7	45.5	37	0.81	-62	1.13	-15
PIF	72.7	0	64.4	0	3.77	0	1.84	0
DPIFR-GS	80	11	68	6	2.34	-38	2.31	25

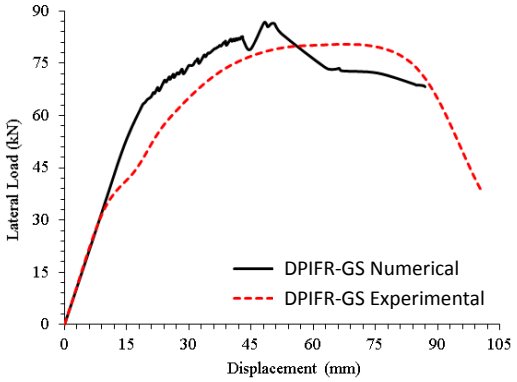

Fig. 19 Comparison of pushover curve and backbone curve of DPIFR-GS

The application of 1.5 mm thick steel plates on the DPIFR-GS specimen was based upon the non-linear static pushover analysis carried out on the retrofitted numerical model of the frame. Fig. 19 shows the comparison of the pushover curve of the retrofitted numerical model with the positive cycle of the backbone curve obtained experimentally. The lateral strength of DPIFR-GS was found to be 80 kN in the experiment and 86 kN in the numerical analysis. Thus, the retrofitted experimental model achieved 93% of the strength predicted numerically. In contrast, the secant stiffness of the numerical model is 3.5 kN/mm, while that of the experimental model is 2.34 kN/mm. Therefore, about 67% of the stiffness, predicted numerically, is achieved in the experiment. The discrepancy in the initial stiffness may have resulted from the higher modulus of elasticity of concrete used in the numerical model. It is to be noted that the modulus of elasticity of concrete is obtained from the following equation (BIS 2000):

$$E = 5000\sqrt{f_{ck}} \quad (1)$$

where f_{ck} = characteristic compressive strength of concrete found experimentally.

Also, a bed-joint failure in mortar in the bottom-most layer of bricks, as observed in the initial stage of loading, may have caused the reduction in secant stiffness in the experimental model.

5.3 Comparison of stiffness degradation of the undamaged and retrofitted frames

Stiffness degradation of the frame is obtained by comparing the secant stiffness of the subsequent hysteretic

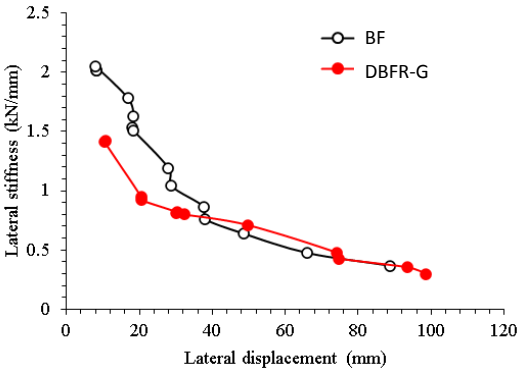

Fig. 20 Stiffness degradation of bare frames

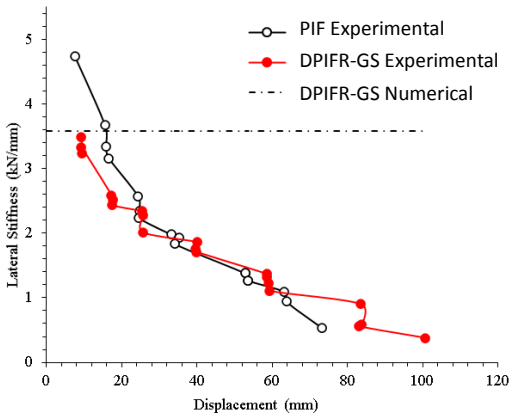

Fig. 21 Stiffness degradation of partially infilled frame

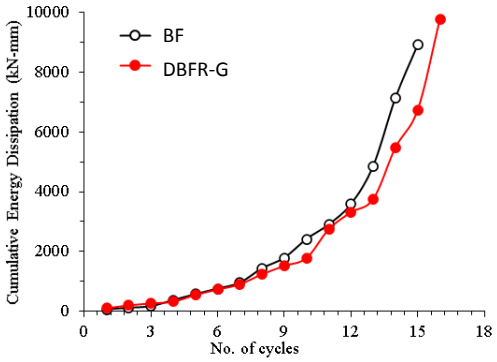

Fig. 22 Comparison of the cumulative energy dissipation of the undamaged (BF) and damaged retrofitted (DBFR-G) bare frames

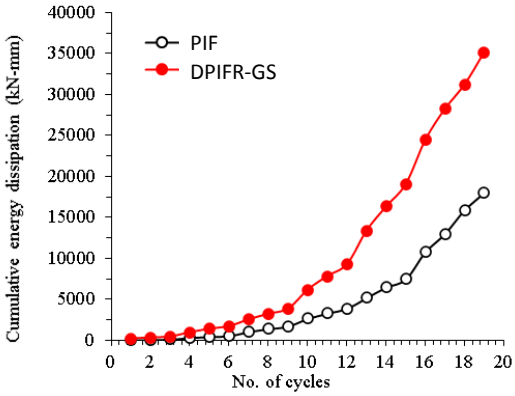

Fig. 23. Comparison of the cumulative energy dissipation of undamaged (PIF) and damaged retrofitted (DPIFR-GS) partially infilled frames

loop. For the undamaged bare frame (BF), the initial stiffness is 2 kN/mm, whereas, for DBFR-G, it is 1.4 kN/mm, i.e., 30% less than the stiffness of the undamaged bare frame. After that, the stiffness degrades gradually with an increase in the displacement cycle, as shown in Fig. 20. The stiffness values of both the bare frames, i.e., BF and DBFR-G match almost exactly after 75 mm displacement, which shows a similar failure pattern.

In the case of the PIF, the initial lateral stiffness is higher with a value of 4.7 kN/mm as compared to DPIFR-GS, which is 3.5 kN/mm, i.e., 25 % less than the stiffness of the undamaged frame (PIF). The stiffness of the PIF drops to 0.5 kN/mm after the 75 mm displacement cycle, whereas for DPIFR-GS, it is still at a value of 1 kN/mm, as shown in Fig. 21. That means the drop in stiffness is more gradual in DPIFR-GS as compared to the PIF because of the extra stiffness provided in the former by the steel plates. Also, in Fig. 21, the initial stiffness of the DPIFR-GS is compared with the target secant stiffness of the pushover curve of the numerically retrofitted PI frame with 1.5 mm steel plates. It can be seen that the secant stiffness of the numerical model and the experimental model (DPIFR-GS) is almost the same.

5.4 Comparison of energy dissipation of the undamaged and retrofitted frames

The energy dissipation is calculated from the area enclosed in the hysteresis loop of each cycle of loading, which is then added to get the cumulative energy dissipation of all the cycles. The cumulative energy dissipation of both the undamaged (BF) and retrofitted (DBFR-G) bare frames are plotted in Fig. 22. It can be observed that both the curves have followed a similar trend. However, the cumulative energy dissipation of the retrofitted frame (DBFR-G) is lesser than that of the undamaged (BF) bare frame because the epoxy grout has made the frame brittle although it increases the capacity of the frame. The cumulative energy dissipation at the 90 mm displacement cycle of the experiments was 6741 kN-mm and 8908 kN-mm for the DRBD-G and BF, respectively. In other words, the retrofitted frame (DRBD-G) showed 25% less energy dissipation capacity as compared to the undamaged frame (BF).

The cumulative energy dissipation of the DPIFR-GS is due to the combination of the RC frame and partial masonry infill wall. However, in the 30 mm displacement cycle, separation of infill wall and column occurs, and also the failure of mortar in the bottom-most layer of bricks leads to the increase in the contribution of the RC frame in the cumulative energy dissipation. At a higher cycle of loading, i.e., at 50 mm, 75 mm, and 100 mm cycles, the steel plates also come into picture along with RC frame and infill frame, which makes the frame more ductile, thereby

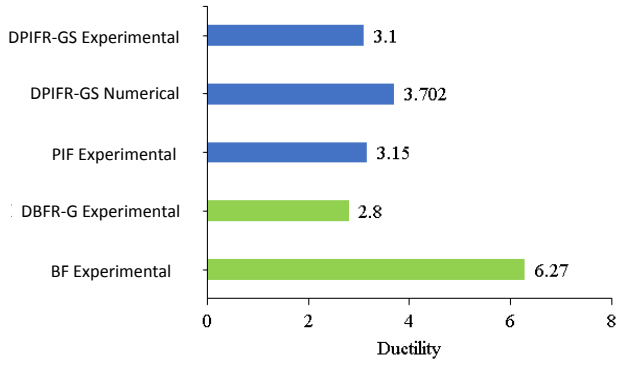

Fig. 24. Ductility value of various frame models

increasing the overall energy dissipation of the frame as shown in Fig. 23. The cumulative energy dissipation of DPIFR-GS and the PIF is 35161 kN-mm and 17990 kN-mm, respectively, i.e., DPIFR-GS showed almost twice the energy dissipation as compared to the undamaged frame. An increase of 25% in energy dissipation capacity was also observed by Sasmal *et al.* (2011) when the damaged beam-column joint was retrofitted by using steel plates, fixed by means of through bolting.

5.5 Ductility of the undamaged and retrofitted frames

Ductility is calculated as the ratio of the failure displacement corresponding to 80% of the ultimate load on the descending part of the load-displacement curve to the yield displacement at 80% of the ultimate load on ascending part of the load-displacement curve (Tawfik *et al.* 2014). The ductility of epoxy repaired bare frame (DBFR-G) was found to be 2.8, which is about 55% lesser than that of the undamaged bare frame (BF) having a ductility value of 6.27 (Fig. 24). The significant reduction in the ductility of DBFR-G as compared to the BF is due to the brittle nature of epoxy injection grout used to retrofit the damaged specimen. However, in the partially infilled frame, the retrofitted specimen (DPIFR-GS) regained a ductility value (98%) as that of the undamaged specimen (PIF). The ductility value of DPIFR-GS and the PIF is 3.1 and 3.15, respectively. The use of ductile steel plates for jacketing played an important role in increasing the ductile behaviour of the partially infilled frame (DPIFR-GS). The numerical analysis of the DPIFR-GS frame showed a ductility value of 3.7, which is almost equal to that of the DPIFR-GS (Fig. 24). The shifting of the captive column effect below the top of masonry infill has increased the slenderness of the column, thereby reducing the shear force on the column, making it less rigid and more ductile.

6. Failure investigation of DPIFR-GS

The visual inspection of the retrofitted partially infilled reinforced concrete frame (DPIFR-GS) indicated only a few minor cracks at the exposed surface of the structure (the region without steel plates) except at the places just below the mid-height of the column (where the steel plate ends).

Fig. 25. Damages in DPIFR-GS

The steel plates also appeared to be undamaged. The extent of the damage in the concrete beneath the steel plates was checked after removing the steel plates. The formation of cracks took place at the mid-height of the column beneath the steel plates due to the captive column effect. However, due to the confinement provided by the steel plates, the cracks were unable to propagate fully. This leads to the shifting of captive column failure in the region where the steel plates end, as shown in Fig. 25 (below the top of masonry infill).

The top beam-column joint (on the leeward side) has also developed many cracks under the steel plates. The diagonal pattern of the cracks is an indication of shear failure at the joints. The cracks were formed at the top of the windward column without affecting the joint region much, as shown in Fig. 25. All of these observations show that the steel plates were effective in sharing the load even after the concrete cracked.

The location and the extent of damage in DPIFR-GS are compared with the location and the state of hinges in the numerical model, as shown in Fig. 25. The shifting of the captive column failure below the top of the masonry infill in the undamaged concrete portion was synonymous with the formation of immediate occupancy hinge below the equivalent diagonal strut in the numerical model. Also, the formation of the immediate occupancy hinge at the top columns are indications of damages in the experimental frame.

7. Retrofitting design procedure

The following design steps can be used for the retrofitting of damaged RC structures:

• Damaged structure type: The damaged RC structure can either be earthquake resistant (ductile detailed) or ordinary structure (non-ductile). In both the cases a thorough failure investigation should be carried out to identify the types of failure (flexural or shear type failure). The severity of the damage should be understood, and based

on the various deflection and serviceability criteria, decision should be made whether the structure is to be demolished or to be retrofitted.

• Evaluation of remaining strength of the structure: If the structure is of ductile nature and has sustained low damages, minor repairing of cracks and structural members would suffice the purpose. However, for non-ductile structures, the residual strength after the damage should be evaluated because retrofitting. This can be done by performing numerical simulations on the simplified model of the structure by conducting equivalent static or dynamic analysis.

• Design of retrofitting scheme: Once the residual strength and stiffness of damaged structure is known, the amount of retrofitting material (steel plate size and thickness) required for regaining the original strength and stiffness can be found out by numerical analysis as discussed elsewhere (Kumawat *et al*. 2020).

• Connection design for application: After the thickness and size of the steel plates required for retrofitting are fixed, the connection of plates to the damaged RC section should be designed, especially from application point of view. The connection design should be such that the steel plates should properly confine the damaged RC section. The connection can be made by bolting or welding.

8. Conclusions

The present study deals with the evaluation of the lateral response of post-earthquake retrofitted reinforced concrete bare frame and RC frame partially infilled with fly-ash bricks. The retrofitting was carried out to regain the undamaged strength and stiffness of the frames. To fulfil this purpose, two different techniques of retrofitting were adopted for the bare frame and partially infilled frame. The bare frame was retrofitted with epoxy injection grouting, while the partially infilled frame was retrofitted with a combination of epoxy injection grouting and steel jacketing. After the retrofitting of the frames, they were subjected to multiple cycles of lateral loading (displacement controlled) till failure of the frame, i.e., about 50% degradation of strength from the peak strength. The following conclusions were drawn from the experimental investigation of the retrofitted frames:

1. This study has shown that, it is possible to regain the original strength of the partially infilled RC frames by adopting judicious techniques of retrofitting, as in this case, it is a combination of epoxy injection grouting and steel jacketing.

2. The epoxy injection grouting alone as a retrofitting scheme was not able to recover the stiffness (38% of undamaged frame), energy dissipation (75% of undamaged frame) and ductility (45% of undamaged frame) parameters of the damaged bare frame.

3. The combination of epoxy injection grouting and steel jacketing retrofitting scheme adopted for damaged partially infilled frame has shown good energy dissipation capacity (200% of undamaged frame), adequate gain in lateral stiffness (75% of its initial stiffness) and ductility values (98 % of undamaged).

4. The steel jackets had confined the damaged concrete sections, thereby pushing the captive column failure into the unretrofitted undamaged part of the frame (just below the top of masonry infill where the steel plate ends). That is, by retrofitting highly stressed zones the frame has shown improved behaviour in terms of strength and stiffness capacity.

Thus, the above study shows that a hybrid retrofitting scheme (epoxy injection grouting and steel jacketing) is more effective in regaining the original capacity of the frame as compared to the individual retrofitting schemes.

The novelty of the work

1. This study proposes a hybrid retrofitting scheme using epoxy injection grouting and steel jacketing technique for damaged partially infilled RC frames. The proposed retrofitting configuration of steel plates and bolting is very easy to implement and effective in regaining the strength and stiffness of the frame.

2. It is the first attempt to study hybrid retrofitting scheme on RC frame partially infilled with fly-ash bricks, which has two-fold environmental merit. (a) The use of fly-ash bricks in infilled frame reduces the use of burnt clay bricks, natural rocks, and concrete blocks, etc., that reduces carbon foot print. (b) It also solves the problem of disposing fly-ash originated from thermal power plants.

Funding

This work was financially supported by the Ministry of Human Resource Development, Government of India.

Reference

Altin, S., Anil, Ö., Kara, M.E. and Kaya, M. (2008), "An experimental study on strengthening of masonry infilled RC frames using diagonal CFRP strips", *Compos Part B-Eng*, **39**(4), 680-693. https://doi.org/10.1016/j.compositesb.2007.06.001.

ASTM (2018), *Standard Test Methods for Compressive Strength of Chemical-Resistant Mortars, Grouts, Monolithic Surfacings, and Polymer Concretes*, ASTM C 579, ASTM International, U.S.A.

Basha, S.H. and Kaushik, H.B. (2016), "Suitability of fly ash brick masonry as infill in reinforced concrete frames," *Mater. Struct*., **49**(9), 3831-3845. https://doi.org/10.1617/s11527-015-0757-5.

BIS (1959), *Method of Tests for Strength of Concrete,* IS:516-1959 (reaffirmed 2004), Bureau of Indian Standards, New Delhi, India.

BIS (1987), *Code of Practice for Structural use of Unreinforced Masonry*, IS:1905-1987 (reaffirmed 2002), Third Revision, Bureau of Indian Standards, New Delhi, India.

BIS (1988), *Methods of Physical Tests for Hydraulic*

Cement, Part 6: Determination of Compressive Strength of Hydraulic Cement (Other than Masonry Cement), IS:4031-PART 6-1988 (reaffirmed 2005), Bureau of Indian Standards, New Delhi, India.

BIS (1992), *Methods of Tests of Burnt Clay Building Bricks, Part 1: Determination of Compressive Strength*, IS: 3495-Part 1-1992 (reaffirmed 2002), Bureau of Indian Standards, New Delhi, India.

BIS (2000), *Plain and Reinforced Concrete - Code of Practice*, IS-456, Bureau of Indian Standards, New Delhi, India.

BIS (2005), *Metallic Materials-Tensile Testing at Ambient Temperature*, IS:1608-2005, Third Revision, Bureau of Indian Standards, New Delhi, India.

Chang, C., Kim, S.J., Park, D. and Choi, S. (2014), "Experimental investigation of reinforced concrete columns retrofitted with polyester sheet", *Earthq. Struct.*, **6**(3), 237-250. https://doi.org/10.12989/eas.2014.6.3.237.

Darbhanzi, A., Marefat, M.S., Khanmohammadi, M., Moradimanesh, A. and Zare, H. (2018), "Seismic performance of retrofitted URM walls with diagonal and vertical steel strips", *Earthq. Struct.*, **14**(5), 449-458. https://doi.org/10.12989/eas.2018.14.5.449.

El-Amoury, T. and Ghobarah, A. (2002), "Seismic rehabilitation of beam–column joint using GFRP sheets", *Eng. Struct.*, **24**(11), 1397-1407. https://doi.org/10.1016/S0141-0296(02)00081-0.

Esmaeeli, E., Barros, J.A., Sena-Cruz, J., Fasan, L., Prizzi, F.R., Melo, J. and Varum, H. (2015), "Retrofitting of interior RC beam-column joints using CFRP strengthened SHCC: cast-in-place solution", *Compos Struct.*, **122**, 456-467. https://doi.org/10.1016/j.compstruct.2014.12.012.

Faleschini, F., Gonzalez-Libreros, J., Zanini, M.A., Hofer, L., Sneed, L. and Pellegrino, C. (2019), "Repair of severely-damaged RC exterior beam-column joints with FRP and FRCM composites", *Compos. Struct.*, **20**(7), 352-363. https://doi.org/10.1016/j.compstruct.2018.09.059.

Garcia, R., Jemaa, Y., Helal, Y., Guadagnini, M. and Pilakoutas, K. (2014), "Seismic strengthening of severely damaged beam-column RC joints using CFRP", *J. Compos. Constr.*, **18**(2), 04013048. https://doi.org/10.1061/(ASCE)CC.1943-5614.0000448.

Hadi, M.N. and Tran, T.M. (2014), "Retrofitting nonseismically detailed exterior beam-column joints using concrete covers together with CFRP jacket", *Constr. Build. Mater.*, **63**, 161-173. https://doi.org/10.1016/j.conbuildmat.2014.04.019.

Hadigheh, S.A., Mahini, S.S. and Maheri, M.R. (2014), "Seismic behavior of FRP-retrofitted reinforced concrete frames", *J. Earthq. Eng.*, **18**(8), 1171-1197. https://doi.org/10.1080/13632469.2014.926301.

Jayaguru, C. and Subramanian, K. (2012), "Retrofit of RC frames with captive-column defects", *KSCE J. Civil Eng.* **16**(7), 1202-1208. https://doi.org/10.1007/s12205-012-1019-5.

Karayannis, C.G. and Golias, E. (2018), "Full scale tests of RC joints with minor to moderate seismic damage repaired using C-FRP sheets", *Earthq. Struct.*, **15**(6), 617-627. https://doi.org/10.12989/eas.2018.15.6.617.

Kaushik, A., Mondal, G. and Dash, S.R. (2018), "Evaluation of lateral response of partially infill walls with fly-ash bricks through experimental study", M.Tech thesis, School of Infrastructure, Indian Institute of Technology Bhubaneswar, India.

Kumawat, S.R., Mondal, G. and Dash, S.R. (2020), "Evaluation of post-earthquake retrofitted partially infilled reinforced concrete frame", M.Tech thesis, School of Infrastructure, Indian Institute of Technology Bhubaneswar, India.

Kumbasaroğlu, A. and Budak, A. (2016), "An experimental study on impact of anchor bars at the steel frames with infilled walls", *Challenge J. Struct. Mech.*, **2**(2), 129-138. https://doi.org/10.20528/cjsmec.2016.06.016.

Kumbasaroglu, A., Yalciner, H. and Aydin, Y.F. (2017), "The effect of infill wall frames on seismic performance levels of reinforced concrete buildings", *Int. Conf. Struct. Eng. Dynam.*, Ericeira, Portugal, July.

Muduli, N., Dash, S.R. and Mondal, G. (2020), "Review of seismic performances of partial infill RC frames", *Adv. Comput. Meth. Geomech.*, **56**, 577-589. https://doi.org/10.1007/978-981-15-0890-5_48.

Park, R. (1989), "Evaluation of ductility of structures and structural assemblages from laboratory testing", *B. New Zealand Natl. Soc. Earthq. Eng.*, **22**(3), 155-166. https://doi.org/10.5459/bnzsee.22.3.155-166.

Ro, K.M., Kim, M.S. and Lee, Y.H. (2020), "Experimental study on seismic retrofitting of reinforced concrete frames using welded concrete-filled steel tubes", *Appl. Sci.*, **10**(20), 7061. https://doi.org/10.3390/app10207061.

Sasmal, S., Ramanjaneyulu, K., Novák, B., Srinivas, V., Kumar, K.S., Korkowski, C., Roehm, C., Lakshmanan, N. and Iyer, N.R. (2011), "Seismic retrofitting of nonductile beam-column sub-assemblage using FRP wrapping and steel plate jacketing", *Constr. Build. Mater.*, **25**(1), 175-182. https://doi.org/10.1016/j.conbuildmat.2010.06.041.

Soltanzadeh, G., Osman, H.B., Vafaei, M. and Vahed, Y.K. (2018), "Seismic retrofit of masonry wall infilled RC frames through external post-tensioning", *B. Earthq. Eng.*, **16**(3), 1487-1510. https://doi.org/10.1007/s10518-017-0241-4.

Srechai, J., Leelataviwat, S., Wongkaew, A. and Lukkunaprasit, P. (2017), "Experimental and analytical evaluation of a low-cost seismic retrofitting method for masonry-infilled non-ductile RC frames", *Earthq. Struct.*, **12**(6), 699-712. https://doi.org/10.12989/eas.2017.12.6.699.

Tawfik, A.S., Mohamed, R.B. and Ashraf, E.Z. (2014), "Behavior and ductility of high strength reinforced concrete frames", *HBRC J.*, **10(**2), 215-221. https://doi.org/10.1016/j.hbrcj.2013.11.005.

Tsonos, A.G. (2008), "Effectiveness of CFRP-jackets and RC-jackets in post-earthquake and pre-earthquake retrofitting of beam-column sub assemblages", *Eng. Struct.*, **30**(3), 777-793. https://doi.org/10.1016/j.engstruct.2007.05.008.

Yuen, T.Y.P., Kuang, J.S. and Ali, B.S.M. (2016), "Assessing the effect of bi-directional loading on

nonlinear static and dynamic behaviour of masonry-infilled frames with openings", *B. Earthq. Eng.*, **14**(6), 1721-1755. https://doi.org/10.1007/s10518-016-9899-2.

Yuksel, E., Ozkaynak, H., Buyukozturk, O., Yalcin, C., Dindar, A.A., Surmeli, M. and Tastan, D. (2010), "Performance of alternative CFRP retrofitting schemes used in infilled RC frames", *Constr. Build. Mater.*, **24**(4), 596-609. https://doi.org/10.1016/j.conbuildmat.2009.09.005.

DK